Experimental evidence for the breakdown of a Hartree-Fock approach in a weakly interacting Bose gas

Jean-Baptiste Trebbia, Jérôme Estève, Christoph I. Westbrook, Isabelle Bouchoule

Experimental evidence for the breakdown of a Hartree-Fock approach in a weakly interacting Bose gas

J.-B. Trebbia,[1,*] J. Esteve,[1,2] C. I. Westbrook,[1] and I. Bouchoule[1]

[1] *Laboratoire Charles Fabry, CNRS et Université Paris 11, 91403 Orsay CEDEX, France*
[2] *Laboratoire de Photonique et de Nanostructures, CNRS, 91460 Marcoussis, France*

We study the formation of a quasi-condensate in a nearly one dimensional, weakly interacting trapped atomic Bose gas. We show that a Hartree Fock (mean-field) approach fails to explain the presence of the quasi-condensate in the center of the cloud: the quasi-condensate appears through an interaction-driven cross-over and not a saturation of the excited states. Numerical calculations based on Bogoliubov theory give an estimate of the cross-over density in agreement with experimental results.

PACS numbers: 03.75.Hh, 05.30.Jp

Since the first observation of the Bose-Einstein condensation in dilute atomic gases, self consistent mean-field approaches (see e.g. [1, 2]) have successfully described most experimental results. For example, the predicted BEC transition temperature T_c agrees well with experiments [3, 4, 5]. In mean-field theory, a Bose gas above T_c is described by a Hartree-Fock (HF) approach in which atoms are considered as independent bosons and one takes into account their interaction by a mean-field potential. As in the ideal gas case, condensation appears when the excited state population saturates. The success of this approach relies on the weakness of the interactions in dilute atomic gases ($\rho a^3 \ll 1$ where ρ is the atomic density and a the scattering length), and also on the absence of very large fluctuations [6]. In a three dimensional gas, it is well known that this latter condition is not fulfilled for temperatures very close to the critical temperature [4] and deviations from mean-field theories are expected. In particular, for a given atomic density, the critical temperature is slightly shifted towards a larger value as compared to its value predicted by mean-field theories [7, 8, 9]. This discrepancy has not been observed experimentally in a trapped 3D Bose gas, mainly because this temperature shift is very small [3, 10].

In this paper, we report on an experimental situation where, although the gas is far from the strong interaction regime, a mean-field Hartree-Fock theory fails to account for our results. More precisely, we present measurements of density profiles of a degenerate Bose gas in an elongated trap with temperatures close to the transverse ground state energy. For sufficiently low temperatures and high densities, we observe the formation of a quasi-condensate at the center of the cloud. We show that, according to the HF theory, a gas with the experimental chemical potential and temperature is *not* Bose condensed, and the HF theory does not reproduce the observed profiles. Thus, the quasi-condensate regime in our experiment is not reached *via* the usual saturation of the excited states. We emphasize that this failure of mean-field theory happens in a situation where the gas is far from the strong interaction regime, which in one-dimension (1D), corresponds to the Tonks-Girardeau gas limit [11, 12, 13], and where mean field theory also fails. To our knowledge, this is the first demonstration of the breakdown of a mean-field Hartree-Fock approach in the weakly interacting limit.

We attribute this failure of the mean-field theory to the nearly 1D character of the gas. It is well known that a 1D homogeneous ideal Bose gas does not experience Bose Einstein condensation in the thermodynamic limit. On the other hand, in the presence of repulsive interactions in the weakly interacting regime, one expects a smooth cross-over towards a quasi-condensate when the linear atomic density becomes much larger than the cross-over density $n_{\mathrm{c.o.}}^{(1\mathrm{D})} = (k_B T)^{2/3}(m/\hbar^2 g)^{1/3}$ [11, 14, 15], where g is the coupling constant and m the atomic mass. This cross-over corresponds to a decrease of relative density fluctuations, the two particle correlation at zero distance $g^{(2)}(0)$ smoothly goes from 2 for the ideal gas to 1 in the quasi-condensate regime. The HF approach fails to describe this cross-over: as for an ideal gas, the thermal gas does not saturate as n increases and one expects for any density a constant correlation value $g^{(2)}(0) = 2$. All the previous results hold for a 1D gas trapped in a harmonic potential at the thermodynamic limit: no saturation of excited states occurs for an ideal gas [16] and the gas smoothly enters the quasi-condensate regime when the peak density goes above $n_{\mathrm{c.o.}}$ [13, 17].

In the experiment we present here, the gas is neither purely 1D nor at the thermodynamic limit: a few transverse modes of the trap are populated and a condensation phenomenon due to finite size effects might be expected [18]. However, we will argue the validity of a scenario similar to that discussed above, in which the gas undergoes a smooth cross-over to the quasi-condensate regime without saturation of the excited states. For our experimental parameters, we also estimate the cross-over density $n_{\mathrm{c.o.}}$ with a three-dimensional Bogoliubov calculation and we find a result in agreement with experimental data.

The experimental setup is the same as [19]. Us-

*Electronic address: jean-baptiste.trebbia@iota.u-psud.fr; URL: http://atomoptic.iota.u-psud.fr/

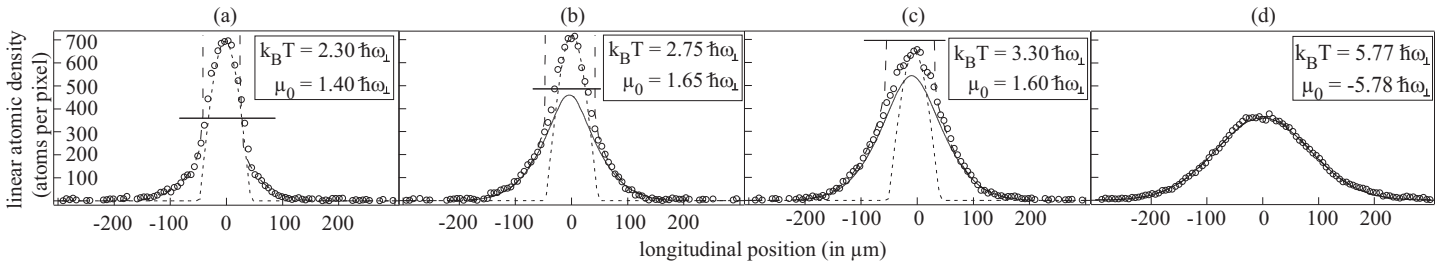

FIG. 1: *In situ* longitudinal distributions for different temperatures (circles). The pixel size is 6.0 μm. Long dashed lines correspond to the ideal Bose gas distribution obtained from a fit to the wings. These fits give the temperature and chemical potential indicated in the insets. The solid lines are the profiles obtained in the Hartree-Fock approximation for the same temperature and chemical potential. The short dashed lines are the Thomas-Fermi profiles with the same peak density as the experimental data. The deviations of the data from the smooth profiles are due to the potential roughness and are seen to be small. Horizontal solid lines give the cross-over density above which the gas enters the quasi-condensate regime, estimated using a Bogoliubov calculation (see text).

ing a Z-shaped wire on an atom chip [20], we produce an anisotropic trap, with a transverse frequency of $\omega_\perp/(2\pi) = 2.75$ kHz and a longitudinal frequency of $\omega_z/(2\pi) = 15.7$ Hz. By evaporative cooling, we obtain a few thousand ^{87}Rb atoms in the $|F = 2, m_F = -2\rangle$ state at a temperature of a few times $\hbar\omega_\perp/k_B$. Current-flow deformations inside the micro-wire, located 150 μm below the atoms, produce a roughness on the longitudinal potential [21]. This roughness is small and we neglect it in the following (see Fig. 1).

The longitudinal profile of the trapped gases are recorded using *in situ* absorption imaging with the same setup as in [19]. The probe beam intensity is about 20% of the saturation intensity and the number of atoms contained in a pixel of a CCD camera is deduced from the formula $N_{\rm at} = (\Delta^2/\sigma)\ln(\mathrm{I}_2/\mathrm{I}_1)$, where $\Delta = 6.0$ μm is the pixel size, σ the effective cross section, and I_1 and I_2 the probe beam intensity respectively with and without atoms. The longitudinal profiles are obtained by summing the contribution of the pixels in the transverse direction. However, when the optical density is large and the density varies on a scale smaller than the pixel size the above formula underestimates the real atomic density [19]. In our case, the peak optical density at resonance is about 1.5, and this effect cannot be ignored. To circumvent this problem, we decrease the absorption cross section by detuning the probe laser beam from the $F = 2 \rightarrow F' = 3$ transition by $\delta = 9$ MHz. We have checked that for detunings larger than δ, the profile remains identical to within 5% up to a normalisation factor. For the detuning δ, the lens effect due to the real part of the atomic refractive index is calculated to be small enough so that all the refracted light is collected by our optical system and the profile is preserved.

To get an absolute measurement of the linear density, we need the effective absorption cross section σ. We find σ by comparing the total absorption of *in situ* images taken with a detuning δ with the total number of atoms measured on images taken at resonance after a time of flight long enough (5 ms) that the optical density is much smaller than 1. In these latter images, the probe beam is σ^+ polarized and the magnetic field is pointing along the probe beam propagation direction. In these conditions, the absorption cross section takes its maximum value $3\lambda^2/2\pi$. We obtain for the *in situ* images taken at a detuning δ, an effective absorption cross section $(0.24 \pm 0.04) \times 3\lambda^2/2\pi$. For samples as cold as that in Fig. 1 (a), the longitudinal profile is expected to be unaffected by the time of flight and we checked that the profile is in agreement with that obtained from *in situ* detuned images within 5%.

Averaging over 30 measured profiles, we obtain a relative accuracy of about 5% for the linear density. A systematic error of about 20% is possible due to the uncertainty in the absorption cross section.

In Fig. 1, we plot the longitudinal density profiles of clouds at thermal equilibrium for different final evaporating knives obtained from *in situ* images. We have compared the density profiles with the expected quasi-condensate density profile with the same peak density. This is obtained using the equation of state of the longitudinally homogeneous case $\mu = \hbar\omega_\perp\sqrt{1+4na}$ [22], and the local chemical potential $\mu(z) = \mu_0 - 1/2m\omega_z^2 z^2$, where n is the linear atomic density, and μ_0 the chemical potential at the center of the cloud. For the two colder clouds (graphs (a) and (b)) in Fig. 1, we observe a good agreement between the central part of the experimental curves (circles) and the Thomas-Fermi profile (short dashed lines) which indicates that the gas has entered the quasi-condensate regime. In [19], we observed the inhibition of density fluctuations expected in this regime.

We extract the temperature and chemical potential of the data from a fit to an ideal Bose gas distribution. For the hottest cloud (graph (d)), such a profile reproduces the data well over its whole extent. For colder clouds however, the ideal Bose gas model should fail in the central part of the cloud where interactions are not negligible. We therefore fit only the wings of the profile. We do this by excluding a number of pixels $N_{\rm ex}$ on either side of the center of the profile. For a given

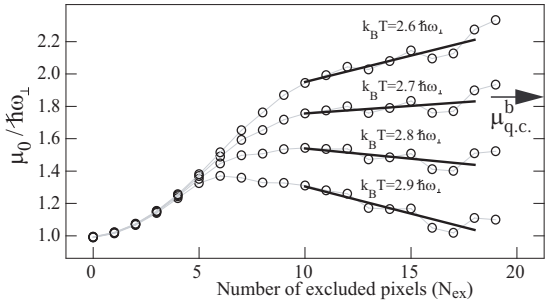

FIG. 2: Chemical potential μ, obtained by fitting the wings a profile (b) to an ideal Bose gas distribution, as a function of the number of excluded pixels $N_{\rm ex}$ on either side of the distribution. The four curves correspond to four different trial temperatures. The sample temperature, found by canceling $d\mu_0/dN_{\rm ex}$ for $N_{ex} > 10$, is $T = 2.75\hbar\omega_\perp/k_B$. The corresponding chemical potential is $\mu_0^b = 1.65\hbar\omega_\perp$. The arrow indicates $\mu_{\rm q.c.} = \hbar\omega_\perp\sqrt{1+4n_0a}$, which is the chemical potential found from the measured peak linear density n_0. The pixel size is 6.0 μm.

temperature, we fit the longitudinal atomic distribution with only the chemical potential as a free parameter. In Fig. 2, we plot the fitted μ_0 as a function of the excluded zone $N_{\rm ex}$ for four different trial temperatures in the case of profile (b). For large $N_{\rm ex}$, μ_0 is about linear in $N_{\rm ex}$. The cloud's temperature is the one for which μ_0 is independent of $N_{\rm ex}$ ($d\mu_0/dN_{\rm ex} = 0$). The deviation from a straight line in Fig. 2 for $N_{\rm ex} > 10$ is mainly due to the roughness of the potential. This deviation contributes about 5% to the uncertainty of T and μ_0. The determination of μ_0 however, is primarily limited by the uncertainty in the total atom number. For profile (b), we find $T_b = (2.75\pm0.05)\hbar\omega_\perp/k_B$ and $\mu_0^b = (1.65\pm0.5)\hbar\omega_\perp$. For the profile (a), the chemical potential and the temperature are not very accurate because the wings are too small and this profile is not analyzed in the following.

Another method to deduce the chemical potential is to use the peak atomic density and the formula $\mu = \hbar\omega_\perp\sqrt{1+4na}$, assuming the gas is well inside the quasi-condensate regime at the center of the cloud. For graph (b), we obtain $\mu^b_{\rm q.c.} = (1.8 \pm 0.2)\ \hbar\omega_\perp$, which is consistent with the value obtained from fits of the wings of the distribution.

We now compute the expected Hartree-Fock profiles of a gas with the same temperature and chemical potential as the experimental data. In this calculation, we assume the relative population of the ground state is negligible (no Bose-Einstein condensation) and the quantization of the longitudinal eigenstates is irrelevant. In such an approach, one can use the local density approximation, and the longitudinal density profile $n(z)$ is found from the equation of state $n_h(\mu, T)$ of a longitudinally homogeneous system using a local chemical potential $\mu(z) = \mu_0 - m\omega_z^2 z^2/2$.

We have to compute $n_h(\mu, T)$, the linear density of a thermal Bose gas trapped in the radial direction and homogeneous in the longitudinal direction. The self-consistent three-dimensional atomic density ρ is the thermodynamic distribution of independent bosons that experience the Hartree-Fock Hamiltonian

$$H_{HF} = \frac{p_z^2}{2m} + H_{\rm kin} + H_{\rm harm} + 2g\rho(r),$$

where r is the radial coordinate, $H_{\rm kin}$ is the transverse kinetic energy term, $H_{\rm harm}$ the transverse harmonic potential. The simplest approach to obtain $\rho(r)$ is to use an iterative method. For each iteration, we numerically diagonalize the transverse part of the Hartree-Fock Hamiltonian H_{HF} to deduce the new atomic density distribution. However, when the interactions become too strong this algorithm does not converge. For the temperature of profile (b), this phenomenon appears for $n_h \geq 320$ atoms per pixel. In this case, we have to use a more time consuming method based on a minimization algorithm. We use the trial function $\rho_{\rm trial}(r) = \sum c_{2p} H_{2p}(r) e^{-r^2/2r_0^2}$ where $H_{2p}(r)$ are Hermite polynomials, and p goes from 0 to 3. We find r_0 and the four c_{2p} coefficients by minimizing the error function $\xi = \int_0^\infty r(\rho'_{\rm trial}(r) - \rho_{\rm trial}(r))^2 dr / \int_0^\infty r\rho^2_{\rm trial}(r)dr$, where $\rho'_{\rm trial}(r)$ is the thermodynamic equilibrium atomic density for $H_{HF}[\rho_{\rm trial}(r)]$. Varying r_0 allows us to obtain good results with only four terms in the expansion. We find ξ less than 10^{-4} meaning that our 5 parameter model describes the transverse Hartree Fock profile well. The linear density $n_h = \int 2\pi r \rho_{\rm trial}(r)dr$ is identical to $n'_h = \int 2\pi r \rho'_{\rm trial}(r)dr$ within 0.5%. In the domain where both methods are valid, we also check that they give the same result. In the presence of longitudinal confinement, the profile is $n(z) = n_h(\mu(z), T)$.

Figure 1 compares the longitudinal profiles obtained with the Hartree-Fock calculation with the experimental data and the ideal gas profile for the graphs (b), (c) and (d). The Hartree-Fock profile for the hotter cloud (graph (d)) is in agreement with data and identical within one percent to the ideal Bose gas prediction. For the slightly colder cloud of graph (c), the Hartree-Fock calculation avoids the divergence in the ideal gas model, but it underestimates the peak density by approximately 20%. For the even colder cloud of graph (b), the discrepancy between the Hartree-Fock profile and the experimental data is even larger (35% at the center).

To validate our Hartree Fock calculations we check *a posteriori* the local density approximation (LDA). The LDA is valid if the population difference between adjacent energy states is negligible. This criterion is met if the absolute value of the effective chemical potential $\mu_{\rm eff} = \mu_0 - \varepsilon_0(\mu)$ is much larger than ΔE, where $\varepsilon_0(\mu)$ is the ground state energy and ΔE the energy gap between the ground state and the first excited longitudinal state. In Fig. 3, we plot the ratio $\mu_{\rm eff}/\Delta E$ as a function of the global chemical potential for the temperature of the graph (b). As long as $\mu_0 < 2.0\hbar\omega_\perp$, $|\mu_{\rm eff}/\Delta E|$ is larger than 15 and for the chemical potential $\mu_0^b = 1.65\hbar\omega_\perp$ deduced from the data $|\mu_{\rm eff}/\Delta E| \simeq 25$. For such a large

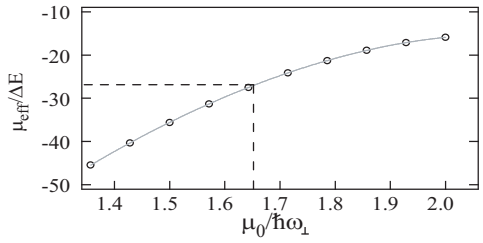

FIG. 3: Ratio between the effective chemical potential and ΔE, the energy splitting between the ground state and the first excited state as a function of the chemical potential for the temperature of profile (b). The dashed lines correspond to the measured chemical potential. The criterion $|\mu_{\rm eff}|/\Delta E \gg 1$ ensures both that the local density approximation is valid for the determination of the density profile and that the relative ground state population is small.

value of $|\mu_{\rm eff}/\Delta E|$, the LDA is expected to be valid.

For this ratio $\mu_{\rm eff}/\Delta E$, we can quantify the error made in the density profile due to the LDA. From the HF calculation, we obtain the energies $E_n(\mu, T)$ of the transverse eigenstates. Assuming the transverse motion adiabatically follows the longitudinal one, we obtain an effective longitudinal Hamiltonian with a potential $V_n(z) = E_n(\mu_0 - m\omega_z^2 z^2/2, T)$ for each transverse mode. The longitudinal density profile is obtained by diagonalization of each effective longitudinal Hamiltonian and summing the resulting thermal profiles. This procedure gives the same longitudinal density profiles as the local density approximation within 5%. We also apply this procedure for HF calculations corresponding to the graphs (c) and (d), and also confirm the validity of the LDA.

In the case of profile (*b*), where the gas enters the quasi-condensate regime at the center, the Hartree-Fock calculation predicts a population of the ground state $N_0 \approx k_B T/(\varepsilon_0 - \mu_0)$ which is smaller than $N_{tot}/100$. Therefore, the Hartree-Fock approach does not predict a saturation of the excited states and fails to explain the presence of the quasi-condensate at the center of the cloud. Note that the local density approximation criterion $|\mu_{\rm eff}| = |\mu_0 - \varepsilon_0(\mu)| >> \Delta E$ also implies a small relative ground state population.

The failure of the Hartree-Fock approach for our experimental parameters is due to the large density fluctuations this theory predicts in a dense, nearly 1D gas. When density fluctuations become too large, pair interactions induce correlations in position between particles which are not taken into account in the Hartree-Fock theory. These correlations reduce the interacting energy by decreasing density fluctuations: the gas enters the quasi-condensate regime.

We now estimate the cross-over density $n_{\rm c.o.}$ at which the gas enters the quasi-condensate regime. For this purpose, we assume the gas is in the quasi-condensate regime and use the Bogoliubov theory to compute density fluctuations. We find *a posteriori* the validity domain of the quasi-condensate regime, which requires that density fluctuations $\delta\rho$ be small compared to the mean density ρ. More precisely, we define $n_{\rm c.o.}$ as the density for which the Bogoliubov calculation yields $\iint (\delta\rho(r))^2/(\rho(r) n_{\rm c.o.})\ d^2r = 1$. We indicate this cross-over density in Fig.1. We find that $n_{\rm c.o.}$ is close to the density above which the experimental profiles agree with the Thomas-Fermi profile.

In conclusion, we have been able to reach a situation where a quasi-condensate is experimentally observed but a HF approach fails to explain its presence. As for purely one dimensional systems, the passage towards quasi-condensate in our experiment is a smooth cross-over driven by interactions. The profiles that we observe require a more involved theory able to interpolate between the classical and the quasi-condensate regime. A Quantum Monte Carlo calculation that gives the exact solution of the many body problem [5, 9] should reproduce the experimental data. In fact, since temperatures are larger than interaction energy, quantum fluctuations of long wavelength excitations should be negligible and a simpler classical field calculation should be sufficient [23, 24].

We thank A. Aspect and L. Sanchez-Palencia for careful reading of the manuscript, and D. Mailly from the LPN (Marcoussis, France) for help in micro-fabrication. The atom optics group is member of l'Institut Francilien de la Recherche sur les Atomes Froids. This work has been supported by the EU under grants MRTN-CT-2003-505032, IP-CT-015714.

[1] A. Griffin, Phys. Rev. B **53**, 9341 (1996).
[2] S. Giorgini, L. P. Pitaevskii, and S. Stringari, J. Low Temp. Phys. **109**, 309 (1997).
[3] F. Gerbier *et al.*, Phys. Rev. Lett. **92**, 030405 (2004).
[4] S. Giorgini, L. P. Pitaevskii, and S. Stringari, Phys. Rev. A **54**, R4633 (1996).
[5] M. Holzmann, W. Krauth, and M. Naraschewski, Phys. Rev. A **59**, 002956 (1999).
[6] L. Landau and E. Lifschitz, in *Statistical physics, Part I* (Pergamon, Oxford, 1980), Chap. 14.
[7] M. Holzmann, G. Baym, J.-P. Blaizot, and F. Laloë, Phys. Rev. Lett. **87**, 120403 (2001).
[8] P. Arnold and G. Moore, Phys. Rev. Lett. **87**, 120401 (2001).
[9] V. A. Kashurnikov, N. V. Prokofév, and B. V. Svistunov, Phys. Rev. Lett. **87**, 120402 (2001).
[10] P. Arnold and B. Tomàŝik, Phys. Rev. A **64**, 053609 (2001).
[11] K. V. Kheruntsyan, D. M. Gangardt, P. D. Drummond, and G. V. Shlyapnikov, Phys. Rev. Lett. **91**, 040403 (2003).
[12] E. H. Lieb and W. Liniger, Phys. Review **130**, 1605

(1963).
[13] D. Petrov, G. Shlyapnikov, and J. Walraven, Phys. Rev. Lett. **85**, 3745 (2000).
[14] C. Mora and Y. Castin, Phys. Rev. A **67**, 053615 (2003).
[15] Y. Castin *et al.*, J. Modern Opt. **47**, 2671 (2000).
[16] V. Bagnato and D. Kleppner, Phys. Rev. A **44**, 7439 (1991).
[17] K. V. Kheruntsyan, D. M. Gangardt, P. D. Drummond, and G. V. Shlyapnikov, Phys. Rev. A **71**, 053615 .
[18] W. Ketterle and N. J. van Druten, Phys. Rev. A **54**, 656 (1996).
[19] J. Estève *et al.*, Phys. Rev. Lett. **96**, 130403 (2006).
[20] J. Reichel, W. Hänsel, and T. W. Hänch, Phys. Rev. Lett. **83**, 3398 (1999).
[21] J. Esteve *et al.*, Phys. Rev. A **70**, 043629 (2004).
[22] F. Gerbier, Europhys. Lett. **66**, 771 (2004).
[23] K. Góral, M. Gadja, and K. Rzązewski, Phys. Rev. A **66**, 051602 (2002).
[24] M. J. Davis and P. B. Blakie, Phys. Rev. Lett. **96**, 060404 (2006).